Reclaiming Motor Functions after Complete Spinal Cord Injury with Epidural Minimally Invasive Brain-Computer Interface

Dingkun Liu, Ph.D.[1#], Yongzhi Shan, M.D., Ph.D.[2#], Penghu Wei, M.D., Ph.D.[2#], Wenzheng Li, M.S.[1], Honglai Xu, Ph.D.[3], Fangshuo Liang, B.S[1], Tao Liu, M.S.[3], Guoguang Zhao, M.D., Ph.D.[2*], Bo Hong, Ph.D.[1*]

[1]Department of Biomedical Engineering, School of Biomedical Engineering, Tsinghua University, Beijing, China.
[2]Department of Neurosurgery, Xuanwu Hospital of Capital Medical University, National Medical Center for Neurological Diseases, Beijing, China.
[3]Neuracle Technology Co., Shanghai, China.

[#] Equal contribution
* Corresponding author

E-mail: hongbo@tsinghua.edu.cn

Abstract:

Background:

Spinal cord injuries significantly impair patients' ability to perform daily activities independently. While invasive brain-computer interfaces (BCIs) offer high communication bandwidth to assist and rehabilitate these patients, their invasiveness limits broader adoption.

Methods:

We developed a minimally invasive BCI system that balances safety and communication bandwidth to restore hand functions of tetraplegia patients. This system enables real-time, precise control of hand movements and hand function rehabilitation. A complete spinal cord injury (SCI) patient with deficit hand functions was recruited in this study.

Results:

The system required less than 10 minutes of calibration time and maintained an average grasping detection F1-score of 0.91 over a 9-month period of home use. With the assistance of the brain-computer interface, the patient can achieve a 100% success rate in object transfer tests, and successfully perform daily tasks involving hand functions. Additionally, the patient showed substantial neurological recovery through consecutive BCI training, regaining the ability to hold objects without BCI assistance. The patient exhibited a 5-point improvement in upper limb motor scores and a 27-point increase in the Action Research Arm Test (ARAT). Improvements in electrophysiological assessments also contributed to enhanced hand control.

Conclusions:

In a tetraplegia patient with complete spinal cord injury, an epidural minimally invasive BCI assisted the patient's hand grasping to perform daily tasks, and 9-month consecutive BCI use significantly improved the hand functions.

Introduction

Spinal cord injuries (SCI) can lead to permanent paralysis of the limbs, especially when the injury occurs in the cervical region, resulting in the loss of motor function in all four limbs. Implantable brain-computer interfaces (BCIs) present a novel solution to help patients regain some motor functions[1,2]. Combined with epidural spinal cord stimulation systems, these interfaces can facilitate functional rehabilitation[3,4]. Current research on implantable BCIs primarily focuses on increasing their communication bandwidth. However, the long-term efficacy and reliability of these systems are often constrained by safety concerns[5,6]. Few studies have investigated how to enhance the safety of implantable BCIs to achieve an optimal balance between communication bandwidth and safety. Additionally, BCIs combined with epidural spinal cord stimulation have been shown to enhance axonal excitability, induce closed-loop electrical activity, and promote active rehabilitation of the brain-spinal cord pathways. This combination can potentially restore voluntary walking abilities in patients[3,7]. However, it remains unclear whether the brain-spinal cord pathways can autonomously recover through BCI-induced sensory and motor feedback without external electrical stimulation.

In our previous research, we designed and validated a brain-computer interface (BCI) system called NEO (Neural Electrical Opportunity) using epidural electrodes and wireless communication in animal models. The NEO system ensures long-term safety and effectiveness through its battery-free, bidirectional design and epidural electrodes that keep the brain tissue intact.

In this study, we utilized the NEO system to develop a long-term hand movement assistance system for a patient with complete C4 spinal cord injury resulting in tetraplegia. We investigated whether neural rehabilitation could be achieved through the coupling of cortical descending control signals and ascending sensory signals at the injury site, without relying on external electrical stimulation.

Methods

The Epidural Minimally Invasive BCI

To create a balanced bridge between bandwidth and safety in brain-upper limb control, we designed an epidural wireless minimally invasive brain-computer interface (BCI) system, named NEO.

The implantable part of the NEO system consists of a titanium alloy implant, a coil, and epidural electrodes. The entire system is sealed with silicone material (Fig. 1b). Two epidural electrode strips are connected to the implant via electrode adaptors, with each electrode strip featuring four contacts capable of both recording and stimulating. These eight electrode contacts have a diameter of 3.2 mm and a center-to-center distance of 8 mm. The system operates at a sampling rate of 1 kHz. It includes two sets of coils: the first set supplies power through near-field coupling, and the second set transmits collected neural signals via Bluetooth.

This design has two main characteristics. First, it employs minimally invasive epidural electrodes. These electrodes, placed on the dura mater, without penetrating the dura, preventing a strong immune response and ensuring long-term effectiveness. Second, the system utilizes bidirectional wireless communication for both power and information transmission (Fig. 1c). Wireless communication reduces the risk of infection by eliminating the need for open wounds. The implant does not contain a battery; instead, it is powered wirelessly via the coils, which also handle bidirectional data transmission. This battery-free design ensures that the device's lifespan is not limited by battery life. While a similar design has been widely adopted in cochlear implants[8], it has not yet been reported in the field of implanted brain-computer interfaces.

Signals are received by a relay station attached to the arm and transmitted to a computer via Bluetooth or WIFI. The computer decodes the patient's motor control signals continuously from the neural data and drives an external pneumatic glove (Fubo Co.) (Fig. 1a, Video 1). When the patient imagines grasping and holding, the pneumatic glove grasps; when the patient imagines relaxing, the glove extends to release the objects.

Study Participant

This study is part of a clinical trial for the implantable closed-loop BCI system (NEO) (clinicaltrials.gov, NCT05920174), which was approved by the Xuanwu Hospital Ethics Committee in April 2023. We recruited a patient in his 50s who suffered a spinal cord injury in a car accident more than 10 years, resulting in limited hand motor function, making grasping, holding, and pinching actions impossible (Video 2). Prior to NEO implantation, the patient underwent a neurological assessment and was diagnosed with complete C4 spinal cord injury (AIS-A, Table S1, Fig. S1).

Informed consent was obtained from the participant with the use of an informed-consent form that was approved by the institutional review board at Xuanwu Hospital of Capital Medical University.

Precise Implantation of Minimally Invasive BCI

To obtain the most informative neural signals related to hand grasping with a minimal number of electrodes, we performed preoperative planning for the BCI electrode implantation using functional MRI (fMRI). Research indicates that the transmission of ascending signals is crucial for SCI rehabilitation[9]. Therefore, our paradigm included fMRI imaging of both active and passive grasping attempts. The active grasping paradigm requires the subject to perform motor imagery based on visual cues, whereas the passive grasping paradigm requires the subject to perceive the sensation of the experimenter assisting him in grasping and releasing. The active grasping paradigm localized the sensory-motor area responsible for the patient's hand, while the passive grasping paradigm assessed the residue ascending sensory signals (Fig. S2). Additionally, we collected CT and structural MRI images of the patient to determine the implantation site.

The significant activation regions were projected from the fMRI onto a 3D model of the cortex, using 3D modeling software to simulate electrode placement (Fig. S2). The position of the implant was determined using skull structure obtained from CT images, selecting an area with suitable

thickness. The final plan was then output to a surgical navigation system to guide the implantation procedure.

The minimally invasive BCI implantation surgery was completed in October 2023. Conducted under general anesthesia, a coronal incision was made on the left scalp to place the internal device, coil, and electrode strips. Following the preoperative plan, a circular window was created in the skull, exposing the dura mater, and the electrodes were sutured onto the dura mater according to the planned positions. The bone flap was then repositioned and secured. A 3-4 mm deep groove was created on the skull surface to embed the titanium alloy implant, which was fixed using bone screws, and the incision was closed. The patient was discharged within 24 hours after all clinical observations were completed.

Postoperatively, we extracted the electrode positions from the patient's postoperative CT images and registered them to the preoperative MRI images, obtaining a map of the eight electrode positions. The first four electrodes were placed above the precentral gyrus, while the latter four were above the postcentral gyrus. Electrodes 2-3 (Brodmann area 6d) in the precentral gyrus and electrodes 7-8 (Brodmann area 1) in the postcentral gyrus covered the most prominently activated hand areas identified by fMRI during hand movement imagination (Fig. 1d, Fig. S2).

Decoding Brain-controlled Grasping Events

Based on our analysis on long-term epidural electrocorticography (eECoG) data (see Results: Long-term Characteristics of Epidural Signals), we confirmed the wideband characteristics of minimally invasive eECoG, which provides spatial resolution between subdural ECoG (sECoG) and scalp EEG. We also observed that the signal amplitude improves with continuous training. To accurately decode the patient's natural grasping movement intention, our decoder needs to integrate multi-band frequency information, restore source space activity, and maintain invariance to signal amplitude over long periods.

Firstly, eECoG features were extracted by combining both spatial and spectral information into a covariance matrix. To address long-term distribution shift in neural features[10], scale-invariant Riemannian metrics was utilized for classification (see Appendix: Spatio-Spectral Riemannian Geometry Decoding Method). Secondly, a hidden Markov model (HMM) was employed to manage the temporal dependencies of continuous grasping actions, ensuring prediction accuracy and stability (Fig. S3 and S4). This approach was compared with two commonly used BCI decoding methods: a linear method, which uses linear spatio-temporal-spectral features[1], and the Common Spatial Pattern (CSP) method[11], which uses multi-band spatial patterns (see Appendix: The Control Decoding Methods).

Assessment of functional and neurological recovery

The regeneration of spinal connections induced by neuroplasticity from electrical activity has been demonstrated in relevant literature[3,12,13]. In this study, descending neural activity was generated by voluntary movement intention from the sensorimotor cortex, while ascending signals from muscle sensory feedback associated with pneumatic hand grasping. Compared with epidural electrical

stimulation over spinal cord to activate downstream muscles[3], our BCI driven process is more likely to trigger bi-directional neuronal coupling at injury sites. To validate this hypothesis, we introduced electrophysiological measurements and neurological scales to evaluate the effectiveness of the rehabilitation.

Somatosensory Evoked Potentials (SEPs) are used to assess sensory information conduction. SEPs are elicited by electrically stimulating peripheral nerves, and the resulting neural activity travels through the sensory pathways to the corresponding areas of the brain, such as the precentral and postcentral gyri. Thus, SEPs reflect the transmission of sensory information from peripheral muscles through the spinal cord to the brain, making them a useful tool for evaluating the extent of spinal cord injury and the progress of recovery[14,15]. SEP testing involves stimulating the median, radial, and ulnar nerves of the patient's right arm (corresponding to C6-T1, C5-C8, and C8-T1, respectively) with a constant current and recording the SEPs from the precentral and postcentral gyri using the NEO epidural electrodes (Fig. 4a).

In this study, we employed two key assessments to quantify the neurological and functional recovery of the subject. The International Standards for Neurological Classification of Spinal Cord Injury (ISNCSCI) scale[16] was used to evaluate the overall neurological status, including motor and sensory capabilities, which is vital for determining the extent of spinal cord damage and subsequent recovery. Additionally, the Action Research Arm Test (ARAT) scale[17] was utilized to assess the finer aspects of hand function, focusing on the subject's ability to handle objects, which is crucial for evaluating the recovery of subtle motor skills of the upper limbs. These scales provided a quantifiable measure for monitoring the improvements in neurological function and hand dexterity over the course of the study.

Results

Long-term Characteristics of Epidural Brain Signals

Generally, brain electrophysiological recordings can be divided into three distinct levels: scalp electroencephalography (EEG), subdural electrocorticography (sECoG), and action potential recordings. These methods vary in safety and signal quality, with EEG being the safest but having the lowest signal quality, and action potential recordings being the most invasive but offering the highest signal quality. We propose that eECoG represents a fourth type, which theoretically provides higher safety than sECoG[6] and is considered minimally invasive. Its spatio-temporal-spectral characteristics are distinct from the other three methods. However, long-term eECoG recordings have been scarce. With NEO BCI system, we obtained substantial amount of eECoG signals for the first time. By analyzing these signals' characteristics in spatial, temporal and spectral domains, we can guide the design of decoding methods for epidural minimally invasive BCI.

Fig. 1e shows the average event-related spectrum perturbation (ERSP) pattern of 1700 trials of imagined hand grasping versus rest by the patient. The spectrum pattern exhibits a typical dual-frequency feature, including low-frequency (15-50 Hz) event-related desynchronization (ERD) and high-frequency (>50 Hz) event-related synchronization (ERS).

We compared the spatio-temporal-spectral characteristics of the patient's epidural ECoG with subdural ECoG datasets[18], the patient's own scalp EEG, and a published EEG dataset[19]. Scalp EEG showed no significant ERSP from the low gamma (>40 Hz) frequency band onwards ($p=0.42$, independent t-test, Fig. 2a). Both epidural and subdural ECoG exhibited low-frequency ERD and high-frequency ERS effects. It is particularly noteworthy that the frequency upper limit of eECoG can exceed 200 Hz, which is significantly higher than that of scalp EEG (Fig. 2a). The power spectral density of eECoG was lower than that of sECoG in different frequency bands but higher than that of scalp EEG in the high-frequency range (20-75 Hz) (Fig. 2b). Spatially, by comparing the relationship between channel correlation and electrode distance, we qualitatively verified the spatial resolution differences among different levels of these three types of recordings. The correlation between EEG channels decreased slowly with increasing electrode distance, indicating lower spatial resolution. The correlation between sECoG channels decreased most rapidly with increasing electrode distance, indicating the highest spatial resolution, with eECoG showing moderate spatial resolution (Fig. 2c).

In contrast to the signal degradation frequently observed in action potential based BCI studies, in the current epidural BCI setting, the quality of long-term eECoG signals improved continuously with training. All electrodes' high gamma (HG) responses significantly increased over nine months of training ($p<0.001$, independent t-test, Fig. 2d), including the electrode no. 8 (Brodmann area 4) which showed the strongest HG response during imagined hand movement. The ERSP effects of electrodes in both the precentral and postcentral gyrus during imagined hand movement also continuously enhanced with training (Fig. 2e-f). Additionally, the HG energy during resting states significantly increased with time ($p<0.001$, independent t-test, Fig. 2h). We continuously measured the epidural electrode impedance to monitor alterations in the patient's intracranial environment post-surgery. The results showed only a slight increase in electrode impedance (<600 Ω), which gradually stabilized after 15 weeks (Fig. 2g).

BCI-assisted Natural Grasping

Based on the characteristics of eECoG, beta band (15-30Hz) and low gamma band (35-50Hz) filtered signal, and high gamma (55-95Hz) power envelope were extracted to train a Riemannian-based classifier. The BCI calibration was made within 10 minutes using a block design paradigm alternating between imagined grasping and resting. For the BCI testing and rehabilitation training task, the patient was instructed to use motor imagery to control a wearing pneumatic hand to move an object from the center of a 3x3 grid to one of the eight surrounding cells (Fig. 3a, Fig. S5). After 10 minutes of calibration, the patient achieved a decoding accuracy of 94% (Chance level: 77%) and a grasp event detection F1 score (see Appendix: Model Training and Evaluation) of 0.8 (Chance level: 0.09). The continuous increase in the patient's high-frequency amplitude of eECoG usually affects the classification accuracy of linear decoders, but has minimal impact on our Riemannian-based classifier[10]. Over nine months, the patient's grasp event F1 score steadily increased, surpassing 0.9 after three months (Fig 3i). The long-term stability of the Riemannian method was superior to both Linear and CSP methods, with the F1 score consistently improving (Fig. 3i) and feature distribution shifts being less pronounced (Fig. S6). After 6 months of training, the subject's capability of grasping with the help of the BCI system was evaluated. In the 3x3 grid test, the success rate was 100% within 10 seconds with BCI grasping, compared to 35% without it

(Fig. 3b-d, 181-185 days after implantation, Video 3). The model's consistent and accurate predictions during the autonomous grasping demonstrate the effectiveness of the BCI system. With BCI assistance, the dwelling time during grasping was distributed between the start and end points, while without assistance, it was mostly around the start point, indicating smoother grasping with BCI assistance (Fig. 3e-f, h). We compared the performance of our system using EEG collected from the subject. The grasp event F1 score for the EEG-based decoder was only 0.16±0.11 (s.d.) (Chance level: 0.07), while for the eECoG it was 0.90±0.06 (s.d.) (Chance level: 0.09) (Fig. 3g). Notably, the average latency decoding was 1.23±0.33s, which is much lower than the EEG based motor imagery BCIs[20,21].

In a home setting, the BCI can assist with various tasks requiring grasping. However, activities like eating and drinking usually elicit significant electromyographic (EMG) noise, which interferes with the decoder. Since the spatial distribution of EMG noise differs from that of grasping movements, the Riemannian geometry method, which is highly sensitive to spatial patterns, can filter out noise without supervised training (Fig. S7). Compared to the Riemannian geometry method, the Linear and CSP methods had a false activation rate (FAR) of 100% during chewing, while the Riemannian geometry method had a FAR of only 20% (Fig. 3j). Using the Riemannian geometry BCI decoder, the patient could perform grasp-related daily tasks such as eating and drinking (Video 4, 267 days after implantation).

Hand Function Rehabilitation and Electrophysiology Assessment

We hypothesis that top-down neural electrical activity from the central and bottom-up sensory feedback from the peripheral during BCI grasping can direct the neuronal projections at the spinal cord injury sites that may facilitate neural rehabilitation[7,22]. Indeed, during nine months of continuous training, significant neurophysiological and functional recovery was observed in the patient. Changes in SEP signals from the radial, median, and ulnar nerves correspond to the recovery of the sensory pathways at different levels of the spinal cord. The strongest and most stable SEP responses were observed in electrode no.5 at Brodmann area 4 (Fig. 4b, Fig. S8). The radial nerve corresponds to spinal segments (C5-T1, mostly C5) above the zone of partial preservation (C5-C7), the median nerve (C5-T1, mostly C6) is near the zone of partial preservation, and the ulnar nerve(C7-T1) is below it[23]. Consequently, it is expected that SEPs from the radial nerve will not show significant change, while SEPs from the median nerve will show some improvement, and SEPs from the ulnar nerve might show less improvement. Over 9 months, the amplitude of SEPs elicited by median nerve stimulation in channel no. 5 increased significantly, whereas the radial nerve did not show significant changes (Fig. 4c). Comparing the first and nineth months, the mean amplitude of early (15-35ms) and late (40-80ms) components of median nerve SEPs increased significantly across most channels. The late component of ulnar nerve SEPs increased significantly in most channels, but the early component did not show a significant increase. The radial nerve showed no significant increase for either component in all channels but channel 4, which showed a significant increase for late component (Fig. 4d, Fig. S9, bootstrap permutation test, FDR corrected, statistical p-values in Table S2).

The patient's neurological scales and hand function assessment corresponded well with the SEP changes. The patient's upper limb motor score on the ISNCSCI scale increased by 5 points over

nine months, with changes concentrated in the C5-C8 segments, and the motor level dropping from C5 to C6. The sensory score increased by 8 points, peaking at 11 points in the fifth month, mostly in the C5-T4 segments (Fig. 5a-b, Table S1). The Action Research Arm Test (ARAT) scale, which evaluates hand functions, including grasp, grip, pinch and gross movements, showed a 16-point improvement in the patient's right hand and a 11-point improvement in the left hand after nine months. The main improvement was in the grasp score, with the trained right hand showing more improvement than the left hand (Fig. 5d, Table S3). For example, in the ARAT grasp test, the patient was able to grasp a 5 cm wooden block faster in the fifth month compared to the third month (3.9 s vs. 6.1 s) and was also able to successfully grasp a 7.5 cm wooden block in the fifth month (Fig. 5c, e-f). The patient completed the ARAT grasping part test before the surgery. Compared to the preoperative results, the grasping speed and success rate for 2.5 cm and 5 cm wooden blocks were significantly improved five months after the surgery (Video 2). It is noteworthy that, due to the patient's use of Baclofen and Pregabalin in the sixth month, there was a sudden decrease in sensory and motor scores.

Discussion

This study presents the first human trial of a wireless minimally invasive epidural BCI system, with which a novel brain-spine rehabilitation pathway was established entirely based on the patient’s intrinsic neural activities. This pathway enabled a patient with a complete C4 spinal cord injury to regain voluntary hand grasping function. Furthermore, active rehabilitation training using the BCI facilitated a prominent recovery of this voluntary grasping function. Significant and consistent improvements were observed in neurological scales, hand function assessments, and electrophysiological tests.

Implantable brain-computer interfaces often face a trade-off between communication bandwidth and safety. Typically, a higher channel number leads to higher bandwidth but lower safety. The wireless minimally invasive epidural BCI system developed in this study, featuring wireless power and transmission with a battery-free, closed-wound design, ensures long-term safety and stability for home use while effectively facilitating hand function restoration and rehabilitation. Although BCIs based on microelectrode implants can achieve similar functions, their long-term stability is limited by issues such as electrode displacement and glial cell encapsulation, necessitating frequent recalibration. Some BCIs using subdural cortical electrodes have been reported to maintain high long-term stability, requiring no recalibration for 2-6 months[24,25]. However, subdural electrodes pose a higher risk of adverse effects such as hematomas, intracranial hemorrhage, brain infarction, and cerebral edema due to direct pressure on brain tissue[6,26]. In contrast, minimally invasive epidural brain-computer interfaces offer significant advantages in long-term stability. The electrodes are placed outside the dura mater, providing structural support without damaging or compressing brain tissues. Consequently, the minimally invasive epidural electrodes exhibit better long-term stability, with signal quality improving over a nine-month period (Fig 2h). Additionally, decoding performance remains stable over nine months with only 10 minutes of calibration (Fig 3i).

In this study, we demonstrated for the first time that a minimally invasive BCI system, relying solely on the patient's intrinsic sensory ascending and motor descending signals, can likely direct the spinal circuit reconstruction, thus to facilitate the rehabilitation of upper limb functions in a patient with complete spinal cord injury. Previous studies have validated the effectiveness of brain-controlled spinal cord injury rehabilitation systems based on this principle[3,27,28], but they largely depend on electrical stimulation of limbs[28] or the spinal cord[3] to induce recovery. Our research confirmed the feasibility of directly using the intrinsic ascending and descending neural activities to facilitate upper limb rehabilitation. Additionally, there is a hypothesis that electrical epidural stimulation of the spinal cord enhances the excitability of spinal nerves, thereby inducing neural circuit remodeling[7,13]. This method complements our approach and could be combined in the future to improve brain-controlled upper limb rehabilitation outcomes.

Our study also established a quantitative assessment method for neural function rehabilitation based on SEP (somatosensory evoked potential) using NEO system. The trend of changes in the amplitude of different SEP components was highly consistent with the patient's rehabilitation progress. At the sixth month, the patient was taking Baclofen and Pregabalin, both of which have inhibitory effects on the central nervous system. These medications exert global suppression on the central system, while SEP, as a primary cortical response to sensory information, is theoretically less affected by such medications compared to higher-level brain activities involved in subjective sensory perception. The results showed that SEP test outcomes were less disturbed than the sensory scores on the ISNCSCI scale, more accurately reflecting the connectivity of spinal neural circuits. Given that similar medications are commonly used by SCI patients, the stability of SEP provides a better assessment of the patient's sensory perception.

This study is a prospective investigation of a novel brain-computer interface, reporting results from a single subject. Consequently, the rehabilitation effects for patients with different injury locations or severities remain uncertain. However, our approach holds potential for application to other spinal cord injury patients. Firstly, the case we reported is an AIS-A level case, representing the most severe level of spinal cord injury. Patients with less severe injuries would have more residual spinal connections, providing higher chance for rehabilitation. Secondly, with nine months of home use, our system is proven to be highly reliable and scalable, with high decoding accuracy and long-term stability. Similar patients can quickly calibrate and use the system at home for long-term, effective rehabilitation training.

Acknowledgement

We thank our volunteer and his family for their commitment and trust. We thank Sichang Chen and Lin Liu from Xuanwu Hospital of Capital Medical University, Yujing Wang and Xiaoshan Huang from Neuracle Technology Co., Zheng Yan from Huaqiao University, Ze'ao Xiong, Ruwei Yao, Yunjing Li, Yujing Lin, Le Yu, Yichao Li from Tsinghua University, and Zhouxingyu Yan from John Hopkins University for their help in this work.

Reference

1. Benabid, A. L. *et al.* An exoskeleton controlled by an epidural wireless brain–machine interface

in a tetraplegic patient: a proof-of-concept demonstration. *Lancet Neurol.* **18**, 1112–1122 (2019).

2. Moses, D. A. *et al.* Neuroprosthesis for Decoding Speech in a Paralyzed Person with Anarthria. *N. Engl. J. Med.* **385**, 217–227 (2021).
3. Lorach, H. *et al.* Walking naturally after spinal cord injury using a brain–spine interface. *Nature* **618**, 126–133 (2023).
4. Samejima, S. *et al.* Brain-computer-spinal interface restores upper limb function after spinal cord injury. *IEEE Trans. Neural Syst. Rehabil. Eng.* **29**, 1233–1242 (2021).
5. Patel, P. R. *et al.* Utah array characterization and histological analysis of a multi-year implant in non-human primate motor and sensory cortices. *J. Neural Eng.* **20**, (2023).
6. Branco, M. P., Geukes, S. H., Aarnoutse, E. J., Ramsey, N. F. & Vansteensel, M. J. Nine decades of electrocorticography: A comparison between epidural and subdural recordings. *Eur. J. Neurosci.* **57**, 1260–1288 (2023).
7. Anderson, M. A. *et al.* Natural and targeted circuit reorganization after spinal cord injury. *Nat. Neurosci.* **25**, 1584–1596 (2022).
8. Zeng, F.-G., Rebscher, S., Harrison, W., Sun, X. & Feng, H. Cochlear Implants: System Design, Integration, and Evaluation. *IEEE Rev. Biomed. Eng.* **1**, 115–142 (2008).
9. Formento, E. *et al.* Electrical spinal cord stimulation must preserve proprioception to enable locomotion in humans with spinal cord injury. *Nat. Neurosci.* **21**, 1728–1741 (2018).
10. Congedo, M., Barachant, A. & Bhatia, R. Riemannian geometry for EEG-based brain-computer interfaces; a primer and a review. *Brain-Computer Interfaces* **4**, 155–174 (2017).
11. Koles, Z. J. The quantitative extraction and topographic mapping of the abnormal components in the clinical EEG. *Electroencephalogr. Clin. Neurophysiol.* **79**, 440–447 (1991).
12. Inanici, F., Brighton, L. N., Samejima, S., Hofstetter, C. P. & Moritz, C. T. Transcutaneous Spinal Cord Stimulation Restores Hand and Arm Function after Spinal Cord Injury. *IEEE Trans. Neural Syst. Rehabil. Eng.* **29**, 310–319 (2021).
13. Moritz, C. *et al.* Non-invasive spinal cord electrical stimulation for arm and hand function in chronic tetraplegia : a safety and efficacy trial. *Nat. Med.* **30**, 18–24 (2024).
14. Kramer, J. K., Taylor, P., Steeves, J. D. & Curt, A. Dermatomal somatosensory evoked potentials and electrical perception thresholds during recovery from cervical spinal cord injury. *Neurorehabil. Neural Repair* **24**, 309–317 (2010).
15. Kramer, J. L. K., Moss, A. J., Taylor, P. & Curt, A. Assessment of posterior spinal cord function with electrical perception threshold in spinal cord injury. *J. Neurotrauma* **25**, 1019–1026 (2008).
16. Rupp, R. *et al.* International standards for neurological classification of spinal cord injury. *Top. Spinal Cord Inj. Rehabil.* **27**, 1–22 (2021).
17. Yozbatiran, N., Der-Yeghiaian, L. & Cramer, S. C. A standardized approach to performing the action research arm test. *Neurorehabil. Neural Repair* **22**, 78–90 (2008).
18. Miller, K. J. A library of human electrocorticographic data and analyses. *Nat. Hum. Behav.* **3**, 1225–1235 (2019).
19. Schalk, G., McFarland, D. J., Hinterberger, T., Birbaumer, N. & Wolpaw, J. R. BCI2000: A General-Purpose Brain-Computer Interface (BCI) System. *IEEE Trans. Biomed. Eng.* **51**, 1034–1043 (2004).
20. Lawhern, V. J. *et al.* EEGNet: A compact convolutional neural network for EEG-based brain-computer interfaces. *J. Neural Eng.* **15**, (2018).
21. Schirrmeister, R. T. *et al.* Deep learning with convolutional neural networks for EEG decoding

and visualization. *Hum. Brain Mapp.* **38**, 5391–5420 (2017).

22. Asboth, L. *et al.* Cortico–reticulo–spinal circuit reorganization enables functional recovery after severe spinal cord contusion. *Nat. Neurosci.* **21**, 576–588 (2018).
23. Grisolia, J. S. & Wiederholt, W. C. Short latency somatosensory evoked potentials from radial, median and ulnar nerve stimulation in man. *Electroencephalogr. Clin. Neurophysiol.* **50**, 375–381 (1980).
24. Luo, S. *et al.* Stable Decoding from a Speech BCI Enables Control for an Individual with ALS without Recalibration for 3 Months. *Adv. Sci.* **10**, 1–12 (2023).
25. Milekovic, T. *et al.* Stable long-term BCI-enabled communication in ALS and locked-in syndrome using LFP signals. *J. Neurophysiol.* **120**, 343–360 (2018).
26. Fountas, K. N. & Smith, J. R. Subdural electrode-associated complications: A 20-year experience. *Stereotact. Funct. Neurosurg.* **85**, 264–272 (2007).
27. Donati, A. R. C. *et al.* Long-Term Training with a Brain-Machine Interface-Based Gait Protocol Induces Partial Neurological Recovery in Paraplegic Patients. *Sci. Rep.* **6**, 1–16 (2016).
28. Jovanovic, L. I. *et al.* Restoration of Upper Limb Function after Chronic Severe Hemiplegia: A Case Report on the Feasibility of a Brain-Computer Interface-Triggered Functional Electrical Stimulation Therapy. *Am. J. Phys. Med. Rehabil.* **99**, e35–e40 (2020).

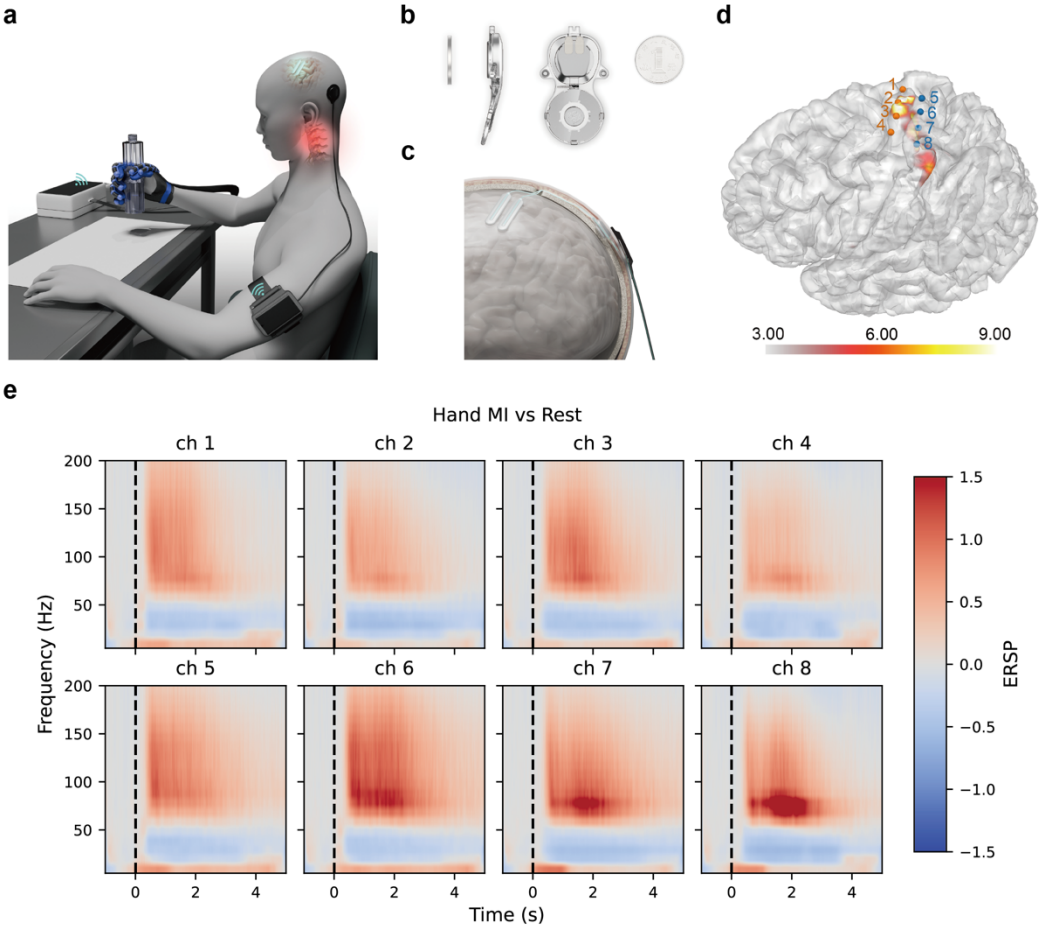

Figure 1 NEO system design and basic signal characteristics. a, Diagram of the NEO brain-computer interface (BCI) system. The NEO BCI system transmits epidural ECoG through a coil to an external device fixed on the patient's shoulder. The external device sends the signals to the host computer, where an algorithm decodes the patient's grasping intention and drives a pneumatic glove to grasp objects. When the patient stops imagining the grasp, the pneumatic glove is driven to open and release the object. b, Structure of the NEO implant. The upper part is the implant, and the lower part is the coil. c, Diagram of the NEO implant implantation position. The coil is magnetically attached through the skin, transmitting signals and power. Electrodes are fixed on the surface of the dura mater and connected to the implant through a skull tunnel. d, Diagram of the patient implantation position. The orange and blue dots represent the electrodes on the precentral and postcentral gyrus, respectively. The heat map overlaying the cortex represents functional MRI activation significance values (negative logarithm of p values). e, Event-related spectral perturbation (ERSP) during imagined grasping. The spectral pattern exhibits a typical dual-frequency characteristic, including low-frequency (15-50 Hz) ERD and high-frequency (>50 Hz) ERS. Hand-MI: Hand Motor Imagery.

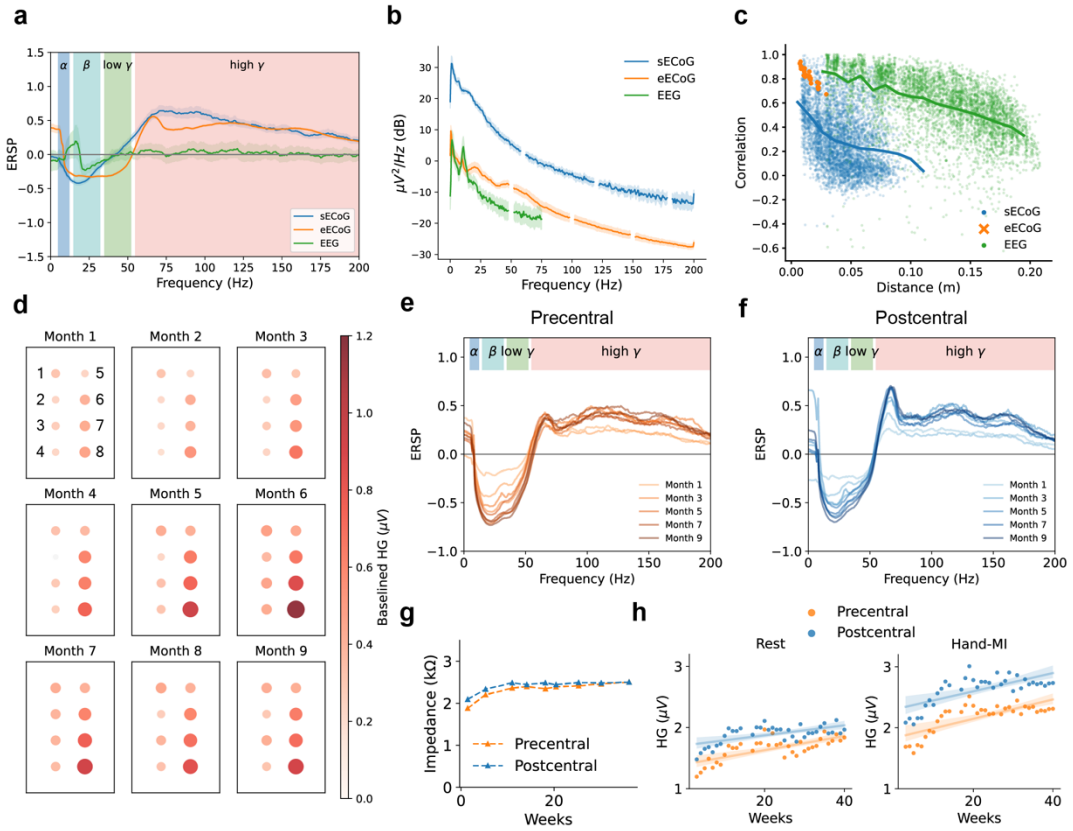

Figure 2 Long-term spatio-temporal-spectral characteristics of epidural signals. a, Comparison of event-related spectral perturbations (ERSP) among subdural ECoG, epidural ECoG, and scalp EEG. Epidural ECoG exhibits an effective frequency band range similar to subdural ECoG. b, Comparison of PSD among the three types of electrophysiological recordings. Subdural ECoG has the highest amplitude, and epidural ECoG has a higher amplitude in the higher frequency band (30-70 Hz) compared to scalp EEG. The PSD excludes the frequency band of power line interference. c, Relationship between channel signal correlation and electrode distance. d, Trend of high-frequency energy (55-95 Hz) spatial patterns of epidural ECoG during imagined hand movements. Long-term training significantly enhances high-frequency activity in the ECoGs of all channels during motor imagery (Month 1 vs. Month 6, $p<0.001$, independent t-test). Channels where the HG response is not significantly greater than zero are marked as gray. e-f, Trend of the average ERSP of precentral and postcentral electrodes, with each curve representing the average ERSP of one month's hand motor imagery data. Both low-frequency ERD and high-frequency ERS gradually increase with training. g, Impedance changes of precentral and postcentral electrodes. h, Trend in high-frequency energy (55-95 Hz, un-baselined) of precentral and postcentral electrodes during rest and hand motor imagery, both showing significant positive correlations (resting: $r=0.67$, $p<0.001$; motor imagery: $r=0.73$, $p<0.001$). In a, b, and c, subdural ECoG data are from the Kai Miller dataset[18]; a and b use scalp EEG from the patient's own recordings; c uses scalp EEG from the BCI2000 dataset[19]. Hand-MI: Hand Motor Imagery. HG: High-Gamma band power.

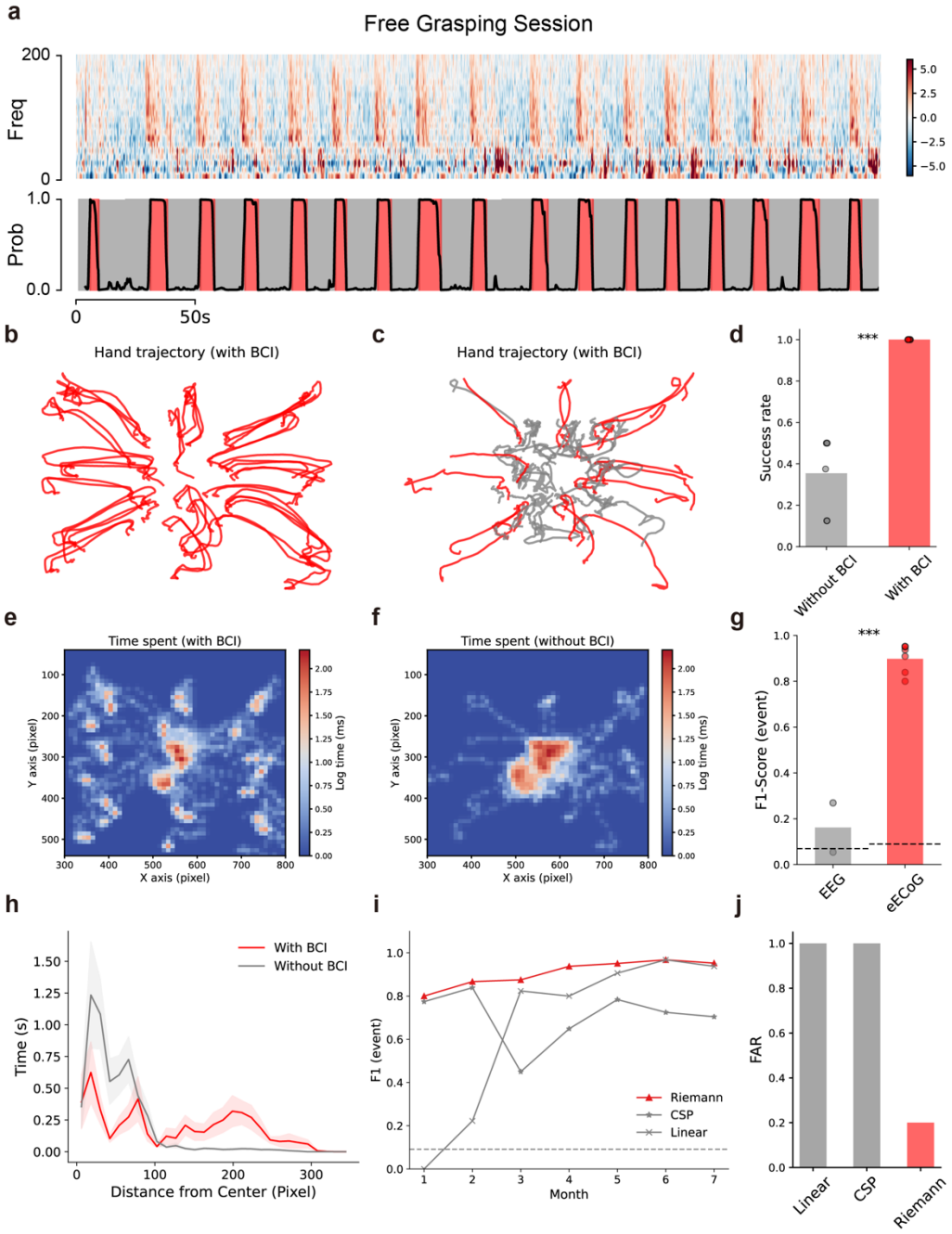

Figure 3 Minimally invasive epidural brain-computer interface (BCI) for motor assistance. a, Example of BCI testing data and decoded confidences. The red shading indicates the time range of the grasping action as determined by the decoder. The grasping action has a high single-trial signal-to-noise ratio. b-c, Hand movement trajectories of the patient performing the BCI testing task with BCI assistance (b) or unaided (c), recorded by a top-down camera and identified by a keypoint detection model. d, With BCI assistance, the patient's success rate of moving the object to the designated position within 10 seconds is 100%, whereas, without BCI assistance, the success rate is only 35%. e-f, Logarithmic spatial distribution of the time spent with BCI assistance (e) or unaided (f). With BCI assistance, the time spent is clustered in the target start and end points, while unaided, the time was mostly spent in the start area. g, Comparison of F1 scores for detecting grasping events using epidural ECoG and scalp EEG. The black dashed line represents the chance level. Epidural ECoG detection F1 scores are significantly higher than

those of scalp EEG. h, Distribution of the relationship between time spent and distance to the central start point. With BCI assistance, the patient can pick up the object and move to the edge more quickly. i, Changes in the F1 score of the decoding algorithm for detecting grasping events over 7 months. The Riemannian geometry-based decoding method shows long-term stability, outperforming the control linear method and CSP method. The gray dashed line represents the chance level. j, Robustness of different models to electromyographic (EMG) noise generated by chewing during daily use. Due to its high specificity to spatial patterns, the Riemannian geometry method shows greater robustness to EMG noise from chewing, which has a different spatial pattern from grasping, compared to the linear method and the CSP method. FAR: False Activation Rate.

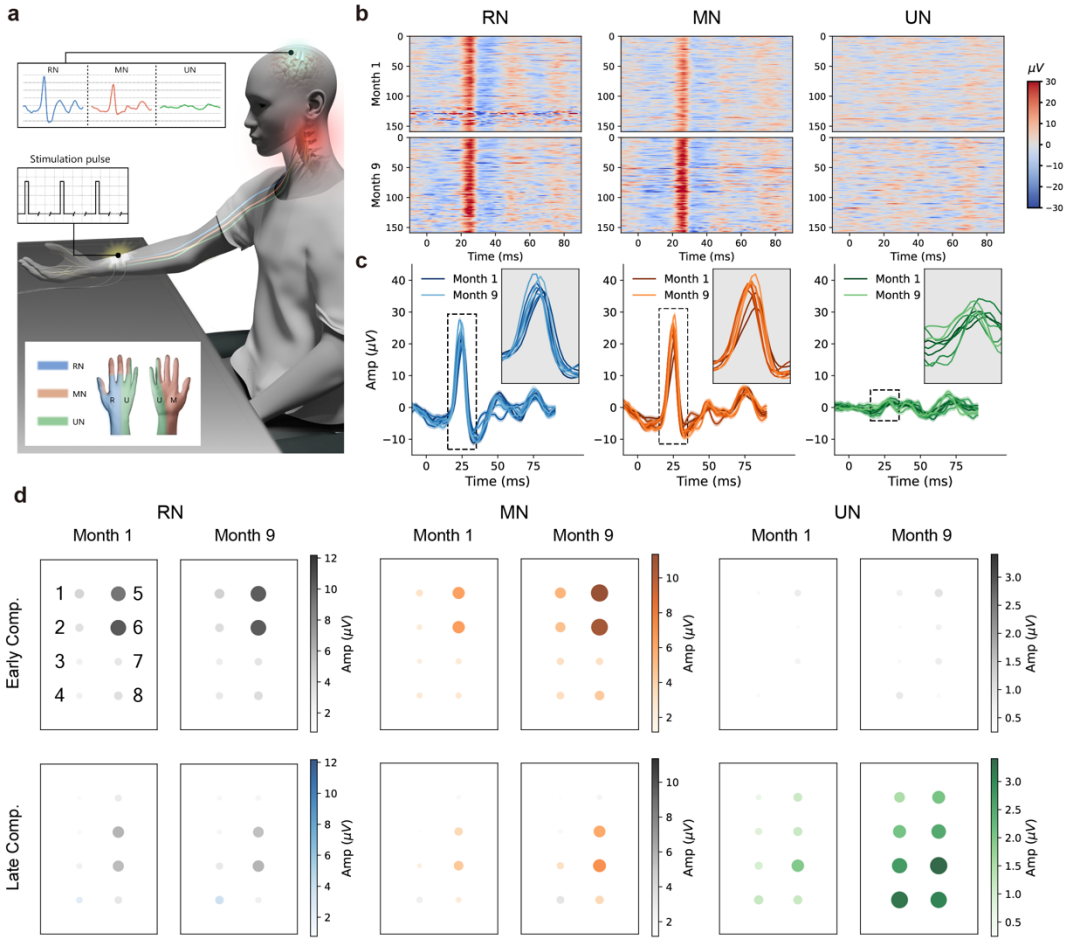

Figure 4 Electrophysiological rehabilitation assessments. a, Diagram of sensory evoked potential (SEP) measurement. Functional stimulators were used to stimulate the patient's radial, median, and ulnar nerves, and SEP activities were recorded from NEO epidural electrodes. b, Trial images of SEP waveforms (channel 5) for the patient's radial nerve (left), median nerve (center), and ulnar nerve (right) at the 1st and 9th months. c, SEP waveforms over 9 months, with colors from dark to light representing SEP waveforms over the 9 months (channel 5). d, Changes in average amplitude of early SEP components (15-35 ms) and late SEP components (40-80 ms) at different electrodes from the 1st month to the 9th month. Electrodes with no significant enhancement ($p>0.05$, FDR-corrected) were marked in gray. MN: median nerve; RN: radial nerve; UN: ulnar nerve.

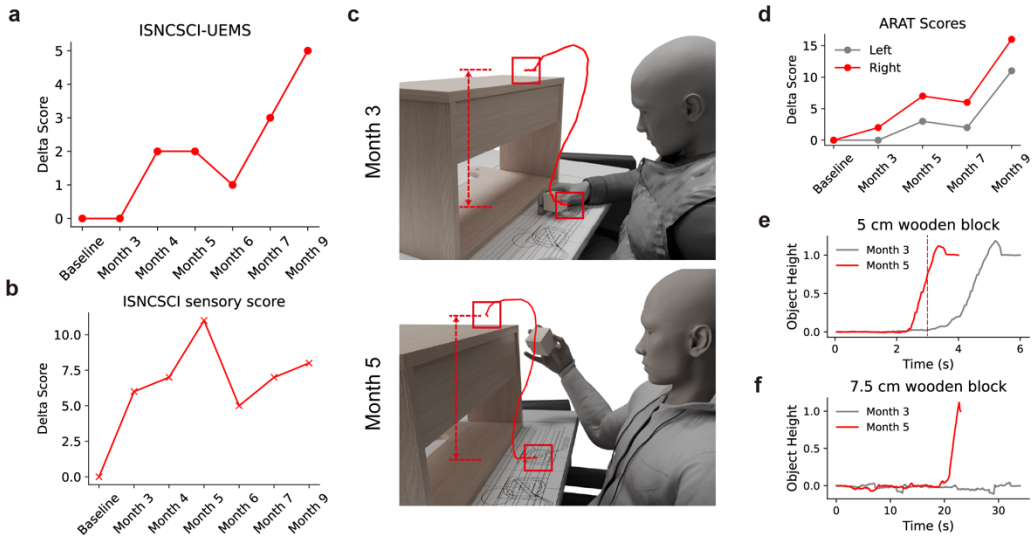

Figure 5 Functional rehabilitation assessments. a, Changes in key muscle strength in the upper limbs according to the ISNCSCI scale. b, Changes in sensory scores of the ISNCSCI scale. Sensory scores encountered a considerable decrease in the 6th month due to the patient's use of antispasmodic medication. c, The patient grasping and releasing a 5 cm block in the Action Research Arm Test (ARAT) test at the 3rd and 5th months. The red curve represents the block trajectory, the boxes mark the start and end points, and the dashed lines indicate the height of the lift. d, Changes in ARAT scores over the course of training. e-f, Curves for lift heights over time of 5 cm and 7.5 cm block grasp tasks in ARAT at the 3rd and 5th months, with the red dashed line indicating the time point shown in h. Trajectories were obtained from video recordings and manually annotated.

Video 1 NEO System Overview.

This video outlines the basic setup of the NEO brain-computer interface (BCI) system. First, the NEO implant is powered on. Next, the pneumatic hand is attached and configured. Once connected to the controller, the NEO system transmits epidural ECoG signals in real-time. Finally, the subject is able to control the pneumatic hand using his thoughts. Link to view online: https://cloud.tsinghua.edu.cn/f/af0fb0644b43496fa4e7/

Video 2 ARAT Grasping Test.

This video demonstrates the subject's improvement in hand function following a 9-month training period. It compares the subject's performance on ARAT tasks before surgery (baseline) and at the 9-month mark for both hands. For the right hand, grasping tasks involving 2.5 cm, 5 cm, and 7.5 cm cubes, as well as a 7.5 cm sphere, are compared between the baseline and 9th month. For the left hand, the grasping task with a sharpening stone is evaluated. Link to view online: https://cloud.tsinghua.edu.cn/f/958b6cad79dd42c4ad12/

Video 3 NEO for Hand Function Assistance.

This video demonstrates how the NEO system assists in hand function. With the help of the BCI system, the subject successfully lifts a bottle of water and moves it to the designated target area. Link to view online: https://cloud.tsinghua.edu.cn/f/e8661aa219b14a988a43/

Video 4 NEO for Independent Home Use.

This video highlights how the NEO system enhances the subject's daily life. Using the NEO system, the subject can independently eat with a customized fork and drink from either a plastic bottle or glass. Link to view online: https://cloud.tsinghua.edu.cn/f/836149c8500441c3abd8/